Understanding the Effects of Tactile Grating Patterns on Perceived Roughness Over Ultrasonic Friction Modulation Surfaces

Shaowei Chu[1] and **Huawei Tu**[2], [1]College of Media Engineering, Communication University of Zhejiang, China, [2]Department of Computer Science and Information Technology, La Trobe University, Australia

Objective: Our study aims to investigate the effects of grating patterns of perceived roughness on surfaces with ultrasonic friction modulation, and also to examine user performance of identifying different numbers of grating patterns.

Background: In designing grating-based tactile textures, the widths of low- and high-friction zones are a crucial factor for generating grating patterns that convey roughness sensation. However, few studies have explored the design space of efficient grating patterns that users can easily distinguish and identify via roughness perception.

Method: Two experiments were carried out. In the first experiment, we conducted a magnitude estimation of perceived roughness for both low- and high-friction zones, each with widths of 0.13, 0.25, 0.38, 0.5, 1.0, 1.5, 2.0, 3.5, and 5.5 mm. In the second experiment, we required participants to identify 5 pattern groups with 2–6 patterns respectively.

Results: Perceived roughness fitted a linear trend for low- or high-friction zones with widths of 0.38 mm or lower. Perceived roughness followed an inverted U-shaped curve for low- or high-friction zones with widths greater than 0.5 mm but less than 2.0 mm. The peak points occurred at the widths of 0.38 mm for both low- and high-friction zones. The statistical analysis indicates that both low- and high-friction zones had similar effects on human perception of surface roughness. In addition, participants could memorize and identify up to four tactile patterns with identification accuracy rates higher than 90% and average reaction time less than 2.2 s.

Conclusions: The relation between perceived roughness and varying widths of grating patterns follows linear or inverted U-shape trends. Participants could efficiently identify 4 or fewer patterns with high accuracy (>90%) and short reaction time (<2.2 s).

Application: Our findings can contribute to tactile interface design such as tactile alphabets and target-approaching indicators.

Keywords: Texture perception, perceived roughness, magnitude estimation, tactile interaction, roughness identification

Address correspondence to Huawei Tu, Department of Computer Science and Information Technology, La Trobe University, Australia. Corresponding Author.
Email: h.tu@latrobe.edu.au
Shaowei Chu, College of Media Engineering, Communication University of Zhejiang, China.
Email: chu@cuz.edu.cn

HUMAN FACTORS
Vol. 0, No. 0, ■■ ■, pp. 1-22
DOI:10.1177/00187208211064025
Article reuse guidelines: sagepub.com/journals-rmissions

INTRODUCTION

Actuator technologies play an important role in improving the user experience of touchscreen interactions on mobile devices. Studies have proven that tactile feedback could alleviate interactive issues such as the "fat finger" problem and no physical sensation of widgets for touchscreen interactions (Hoggan et al., 2008; Luk et al., 2006). Recent studies have been focused on the use of tactile feedback in application scenarios such as conveying tactile alphabets (Liu & Dohler, 2020), text typing (Hoggan et al., 2008), target acquisition (Henderson et al., 2019), drag & drop operation (Gordon & Zhai, 2019), accessibility (Bateman et al., 2018), eyes-free interaction (Chen et al., 2014), and notification awareness (Saket et al., 2013). Therefore, tactile feedback has become a significant component on touchscreen mobile devices.

To enrich the diversity of tactile feedback on touchscreen mobile devices, researchers have investigated how to develop techniques that can render tactile information on touchscreens. Electrostatic and ultrasonic actuation are two emerging techniques that provide dynamic friction on the touchscreen (Basdogan et al., 2020). For the electrostatic actuation technique, an electrostatic force increases the friction between finger and

surface by electroadhesion (Bau et al., 2010). For the ultrasonic actuation technique, piezoelectric motors are employed to generate ultrasonic frequencies of vibrations on touch surfaces, so that a reduction in friction between the sliding finger and surface can be created via the effect of squeeze film (Casiez et al., 2011). The advantage of electrostatic and ultrasonic actuation techniques is that they could provide sophisticated feedback to the fingertip rather than the entire hand as provided by mechanical actuators. Such fine-grained tactile feedback could generate surface roughness to simulate various textures of real objects on touchscreens (Vardar et al., 2017).

Previous studies have explored the perceptual mechanism of how people perceive the roughness of generated surface textures. As for perceived roughness over real textures, Katz (Katz, 1989) proposed the *duplex theory of tactile texture perception* to explain the perceptual mechanism of finely and coarsely textured surfaces. For fine textures with a spatial period of less than 0.2 mm, texture discrimination only takes place in the movement condition, and Pacinian corpuscle afferents mediate the perception. For coarse textures within a spatial period larger than 0.2 mm, roughness features are carried from the skin to the brain mostly by slowly adapting afferents system (Blake et al., 1997; Connor et al., 1990). The magnitude estimation data indicated that the perceived roughness of coarse textures was generally a power function of spatial period, and the perceived roughness tended to follow an inverted U-shape trend with the increase of groove width (Hollins & Bensmaa, 2007; Hollins & Risner, 2000; Lederman, 1974; Taylor & Lederman, 1975).

Compared to the many studies on real textures, relatively fewer studies have been done on perceived roughness over virtual textures. Previous studies have investigated texture discrimination, magnitude estimation and identification to understand the perceptual mechanism over virtual textures. For example, Biet et al. (M. Biet et al., 2008) explored grating design using the spatial periods (SPs) and Weber fraction to measure the discrimination thresholds. In their study, the participants distinguished a difference of 8.96% in the spatial periods (SPs) of the two patterns presented to them. Saleem et al. (2020) studied step changes in frictional gratings on an ultrasonic friction surface. Their results showed a step fall in friction followed by a step rise in friction could be identified more easily than the reverse order. They also reported that a relative difference of 14% in spatial period was required to discriminate two grating patterns. Klatzky et al. (2019) investigated the detection and identification of frictional patterns in coarse fingerprint, fine fingerprint, and star patterns rendered by electrostatic actuation. Their results showed that participants could identify the patterns in around 1 second with a miss rate of 3.9% and a false alarm rate of 4.1% but with a very low identification accuracy (36.1%). The low accuracy may be because of the mismatching between scaled stimulus images and frictional patterns, difficulty in mapping edge distributions on the fingertip to a visual display, and noise caused by both finger moving and friction rendering of the haptic device. Although these studies have investigated the perception of virtual texture features, they provide limited information on perceived roughness in terms of perceptual mechanisms. An exception is a study by Vardar et al. (Vardar et al., 2017), which looked into roughness perception of virtual textures using a magnitude estimation method. They found that when groove width varied from 0.125–7.5 mm, the roughness perception followed an inverted U-shape trend with respect to groove width. However, they only varied ridge width but kept groove width constant. It is unclear whether and how low- and high-friction zones with different widths affect human perception of perceived roughness. As shown in Figure 1, the virtual square gratings are composed of high-friction zones and low-friction zones. With varying widths of low- and high-friction zones, various gratings can be obtained to convey different sensations to sliding finger on friction surfaces. In addition, Vardar et al. (2017) investigated perceived roughness using the device with electrostatic actuation, but did not consider devices with ultrasonic actuation. According to Gueorguiev et al. (2019), ultrasonic and electrostatic devices may differ in the sharpness of the virtual gratings' edges because of their

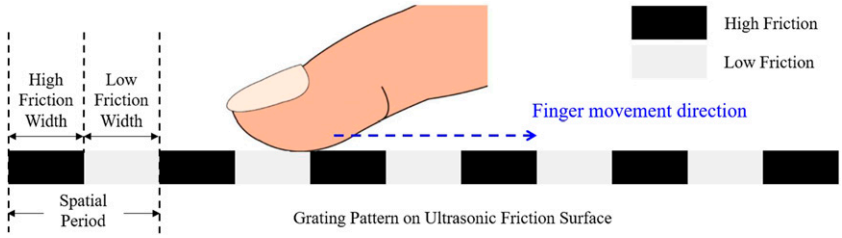

Figure 1. The grating pattern of texture with low-/high-friction zones (black: high-friction zones; white: low-friction zones) for conveying roughness while a finger moves across the friction zones in the left or right direction.

disparity in the time needed for the ultrasonic wave to establish itself. The sharpness of the edges could impact roughness perception, which in turn may influence the perceptual mechanism. Therefore, the results of Vardar et al. (2017) may not be directly generalized to roughness perception over virtual textures generated by ultrasonic haptic devices.

We need to address the following questions to achieve a better understanding of perceived roughness over virtual textures with ultrasonic haptic devices. How can we select a group of grating patterns that are perceived differently from each other? And what is the maximum number of tactile patterns rendered by ultrasonic friction surfaces that could be easily distinguished and identified, particularly in the absence of visual clues? What is the user performance of identifying grating patterns in terms of accuracy and reaction time? These questions are crucial in designing tactile-based interfaces. We must understand user performance in perceiving the roughness of tactile patterns over ultrasonic friction surfaces. On the basis of the understanding of human capabilities, we then can design efficient tactile patterns and develop new tactile applications.

In this study, we conducted two experiments with an ultrasonic haptic device to address the above questions. In experiment 1, we investigated the effects of widths of low- and high-friction zones on perceived roughness. Magnitude estimation of perceived roughness was conducted for both low- and high-friction zones, each with the widths of 0.13, 0.25, 0.38, 0.5, 1.0, 1.5, 2.0, 3.5, and 5.5 mm. In experiment 2, we examined participants' ability of grating pattern identification. Five pattern groups with different numbers of patterns (i.e., 2–6) were used for the experiment. Results showed that both low- and high-friction zones in grating pattern design played similar effects on human perception of grating pattern roughness. Besides, participants could identify four or fewer patterns with an accuracy rate higher than 90% and an average reaction time of less than 2.2 s.

Our work offers the following contributions:

1. A systematical investigation into the human ability to perceive grating pattern roughness over ultrasonic frictional surfaces.
2. Exploring efficient designs of grating patterns to render surface roughness.
3. Performance evaluation on user capability of perceiving and identifying grating patterns based on roughness.
4. Design implications for tactile interfaces by considering the human ability to identify grating patterns.

EXPERIMENT 1: ROUGHNESS PERCEPTION

The goal of this experiment was to investigate how users perceive roughness with the grating design which is based on the combinations of *low-friction* and *high-friction zones*. The following questions were the main focuses of this experiment.

Q1 What is the relation between perceived roughness and varying widths of *low-friction* and *high-friction* zones? Existing studies have investigated the human perception of roughness on virtual textures (Unger et al., 2011; Vardar

et al., 2017). However, they only controlled a single parameter, either *low-friction* or *high-friction*. We aimed to evaluate the effects of the combination of both *low-friction* and *high-friction* zones on perceived roughness. Intuitively, perceived roughness would vary across different combinations of low-friction and high-friction zones. We would like to find out the perceived roughness trends for varying widths of *low-friction* and *high-friction* zones.

Q2 Would low-friction and high-friction zones equally contribute to perceived roughness? If not, would low-friction zones have a greater impact on perceived roughness than high-friction zones, or vice versa? Answering these questions could deepen our understanding of roughness perception and also benefit grating pattern design.

Apparatus

We used a TPad phone in the experiment, which was introduced through an open-source project (Figure 2). The device was assembled on the basis of an Android smartphone. The device provided dynamic frictions on the touchscreen by using air squeeze film damping (M Biet et al., 2007) which could generate ultrasonic vibration to adjust the friction of the touchscreen. When vibration is not actuated, the surface friction is the same as a glassy surface; otherwise, the surface friction is reduced by the squeeze film effect. The amount of decrement can be controlled by an alternating voltage that is applied to the vibration actuator embedded in the TPad. This technology has a great potential for mobile applications because it provides unique roughness sensations to fingertip at a low cost and with high accessibility (Birnholtz et al., 2015; Hightower et al., 2019; Mullenbach et al., 2014; Mullenbach et al., 2013).

The device had a 10.4 cm × 5.85 cm 4.7 inch touchscreen, a display resolution of 720 × 1280 pixels. The dimensions of the device were 16.5 cm in length, 7.0 cm in width, and 1.0 cm in height. The weight was approximately 160 g. The default working parameter of the TPad in the experiment was a piezoelectric operation frequency of 40 kHz to produce the strongest feedback.

A TPad application was developed in Java for the experiment, as shown in Figure 2. We asked participants to maintain finger movement speed

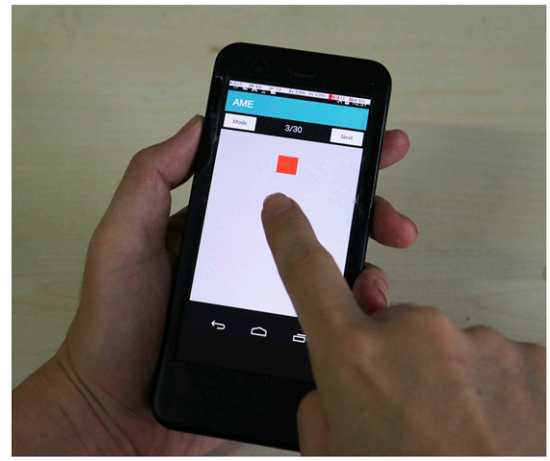

Figure 2. The TPad phone and the experimental interface. The red rectangle moves left and right in the horizontal direction at a constant velocity of 50 mm/s to guide the participant's finger velocity. The participant can perceive dynamic friction on the gray area of the screen.

at approximately 50 mm/s during the experiment by following a target moving left and right on the screen. We selected this speed based on (Vardar et al., 2017).

Participants

A total of 12 students (6 male, 6 female) in the local university were recruited for the experiment. The mean age of the participants was 20.9 years (SD = 1.2). All participants had at least four years of experience in using touchscreen mobile devices, but none of them had experience in using a tactile device such as the TPad. After the experiment, each participant was paid 50 Chinese yuan for the participation.

Grating Pattern Design

A grating pattern consists of two-zone types: *low-friction zone* and *high-friction zone*. The width of the *low-friction zone* and the width of the *high-friction zone* are represented as *LW* and *HW* respectively, as shown in Figure 1. Different (*LW*, *HW*) combinations produce various grating patterns, accordingly may provide users different levels of perceived roughness.

According to (Vardar et al., 2017), we selected nine width values for *LW* and *HW*: 0.13, 0.25, 0.38, 0.5, 1.0, 1.5, 2.0, 3.5, and 5.5 mm. Note that, we excluded the largest width (7.5 mm) used in (Vardar et al., 2017). Such a width resulted in a very low magnitude of perceived roughness in our pilot study, as participants could hardly discriminate the difference of patterns that contained this value as either *LW* or *HW*. We then assigned the nine width values to *LW* and *HW*, respectively, resulting in 81 (9 × 9) grating patterns.

Experiment Design

The experiment was a within-subject repeated measures design. The *independent variable* was the grating patterns with 81 conditions.

The *dependent variable* was the magnitude of perceived roughness. We adopted abstract magnitude estimation (AME) (Gescheider & Hughson, 1991) to measure the relation between grating patterns and perceived roughness. Many well-established psychophysical research methods have been proposed to understand the correlation between changes in physical stimuli and associated sensation (Jones & Tan, 2013; Lederman, 1974). Of those, we chose to use AME which requires users to estimate the strength of stimuli by assigning numbers to them. Because this method does not set a predefined maximum and minimum, users are capable of making unbiased numerical judgments of psychological magnitude as they are permitted to use their own natural units (Gescheider & Hughson, 1991). AME is suitable for an experimental design in which the presence of the target experience is unknown. The result of AME will allow us to create response curves that show how a change in *LW* or *HW* influences perceived roughness.

Procedure

The experimental procedure had three steps:

1) The experimenter described grating pattern roughness to the participants by showing different pairs of (*LW*, *HW*) patterns on the TPad. The experimenter asked participants to sense these patterns and understand the difference between grating pattern roughness and motor vibration by the TPad.
2) The experimenter showed participants a (*LW*, *HW*) = (a, b) pattern (a and b represent one of the nine values of *LW* and *HW* used in the experiment) and asked them to feel it and give a magnitude value to quantify the perceived roughness. The magnitude value was expected to fall between 1 and 100. However, according to the AME method, the experimenter did not ask the participants to restrict the reported magnitude values to any limit, and values lower than 1 or greater than 100 were also acceptable.
3) Participants were asked to sit in a chair to perform the task with the index finger of the dominant hand while holding the device with the non-dominant hand. They could perceive each pattern as many times as they wanted by drawing either left or right flick gestures with the index finger of their dominant hand. The 81 patterns with two repetitions were randomly shuffled. In each perception task, participants perceived the pattern and reported their estimated magnitude of roughness to the experimenter for recording. The participants were instructed to wash their hands with soap to remove residual oils on their skin, and wore noise-canceling headphones to avoid the disturbance of audio clues on their perception. Participants rested every 30 trials during the experiment.

The experiment consisted of 81 patterns × 2 repetitions × 12 participants = 1944.

The experiment lasted for an average of 60 minutes for one participant.

RESULTS

As mentioned earlier in this section, we aimed to understand the relationship between perceived roughness and varying *LW* and *HW*. To this end, we first plotted the data AME to check varying trends of perceived roughness with regard to *LW* and *HW* changes. Afterward, we statistically analyzed the effects of *LW* and *HW* on perceived roughness. And finally, we proposed a method of how to select grating patterns that are most distinctive from each other.

Plot of the Perceived Roughness

The collected data included 1944 magnitudes of perceived roughness on 81 patterns. Most of

the magnitude data (99.8%) were fall within 1–100. Ten (0.2%) magnitudes exceeded 100 (the maximum was 110), but no magnitude was lower than 1. For data plot and statistical analysis, the roughness magnitudes were normalized using the following formula according to (Vardar et al., 2017).

$$r' = \frac{r - min}{\max - min} \quad (1)$$

Where r represents the magnitude of perceived roughness, *min* and *max* represent the minimum and maximum of individual perceived roughness magnitudes, respectively, and *r'* represents the normalized value.

Our analysis was conducted based on the plot analysis method in previous studies (İşleyen et al., 2020; Vardar et al., 2017). Such a method has been used to investigate perception mechanisms. It was originally used in analyzing magnitude estimation results of perceived roughness over real grooved surfaces (Lederman, 1974). The plot analysis is useful to obtain varying trends with respect to gratings' spatial period. And the linear or quadratic trends can quantify the relationship between widths of friction zones and perceived roughness.

The data were then categorized into nine groups and plotted against nine conditions to observe their trends (Figure 3a–i). For example, Figure 3a shows two lines. The solid one illustrates that the *low-friction zone* keeps constant at 0.13 mm width and the *high-friction zone* varies from 0.13 mm to 5.5 mm. The dotted line shows the *high-friction zone* keeps constant at 0.13 mm width and the *low-friction zone* varies from 0.13 mm to 5.5 mm. The cases for 0.25 mm–5.5 mm are shown in Figure 3b–i respectively.

The Shapiro–Wilk test showed that magnitude data were not all normally distributed, so the Friedman test was used to analyze the results of perceived roughness. The Wilcoxon signed-rank test was used for *post hoc* analysis.

On the whole, the magnitude of perceived roughness generally declined with increasing either width of *low-friction* zone or *high-friction* zone value. The perceived roughness appeared linear or quadratic trends with varying widths of *LW* and *HW* in different conditions. From Figure 3a and b, it can be seen that there were good linear fits on perceived roughness for both *LW* and *HW* constant cases ($H(8) = 93.81$, $p < .001$, $R^2 = 0.9758$ and $H(8) = 93.94$, $p < .001$, $R^2 = 0.9845$ for solid and dotted lines, respectively, in Figure 3a, and $H(8) = 92.76$, $p < .001$, $R^2 = 0.9441$ and $H(8) = 91.84$, $p < .001$, $R^2 = 0.9489$ for solid and dotted lines, respectively, in Figure 3b). *Post hoc* analysis revealed that for each line, almost all of the widths were significantly different from each other (all $p < 0.05$) when the varying width larger than 0.25 mm except the width of 0.5 versus 1.0 mm in Figure 3b dotted line ($p = 0.167$).

For the 0.38 mm condition shown in Figure 3c, there was still good linear fit for *LW* and *HW* conditions ($H(8) = 86.36$, $p < .001$, $R^2 = 0.857$ and $H(8) = 82.95$, $p < .001$, $R^2 = 0.8776$, respectively), as shown in solid and dotted lines. The *post hoc* analysis showed that all varying widths greater than 1.0 mm were significantly different from each other (all $p < 0.05$).

The perceived roughness followed an inverted U-shape trend when the varying width reached 0.5 mm but less than 2.0 mm as shown in Figure 3d–g. All the solid and dotted lines show good quadratic fits ($H(8) = 86.76$, $p < .001$, $R^2 = 0.974$ and $H(8) = 86.13$, $p < .001$, $R^2 = 0.979$ in Figure 3d; $H(8) = 80.72$, $p < .001$, $R^2 = 0.969$ and $H(8) = 75.44$, $p < .001$, $R^2 = 0.969$ in Figure 3e; $H(8) = 71.07$, $p < .001$, $R^2 = 0.937$ and $H(8) = 63.44$, $p < .001$, $R^2 = 0.9613$ in Figure 3f; and $H(8) = 60.87$, $p < .001$, $R^2 = 0.8813$ and $H(8) = 64.34$, $p < .001$, $R^2 = 0.9062$ in Figure 3g). On the inverted U-shape curves, all peak points occurred at the widths of 0.38 mm. The *post hoc* analysis revealed that all the 0.38 mm peak points were significantly different from their corresponding 0.13 mm and 5.5 mm cases (all $p < 0.05$). These statistical results confirmed the nature of the inverted U-shape trend of perceived roughness.

Figure 3h and i also show an inverted U-shape trend for the varying width on 3.5 mm and 5.5 mm conditions; however, the trends were flat ($H(8) = 38.33$, $p < .001$, $R^2 = 0.9055$ and $H(8) = 51.96$, $p < .001$, $R^2 = 0.7924$ for solid and dotted lines respectively in Figure 3h, and $H(8) = 42.36$, $p < .001$, $R^2 = 0.7803$ and $H(8) = 14.41$, $p = 0.04$, $R^2 = 0.6932$ for solid and dotted lines

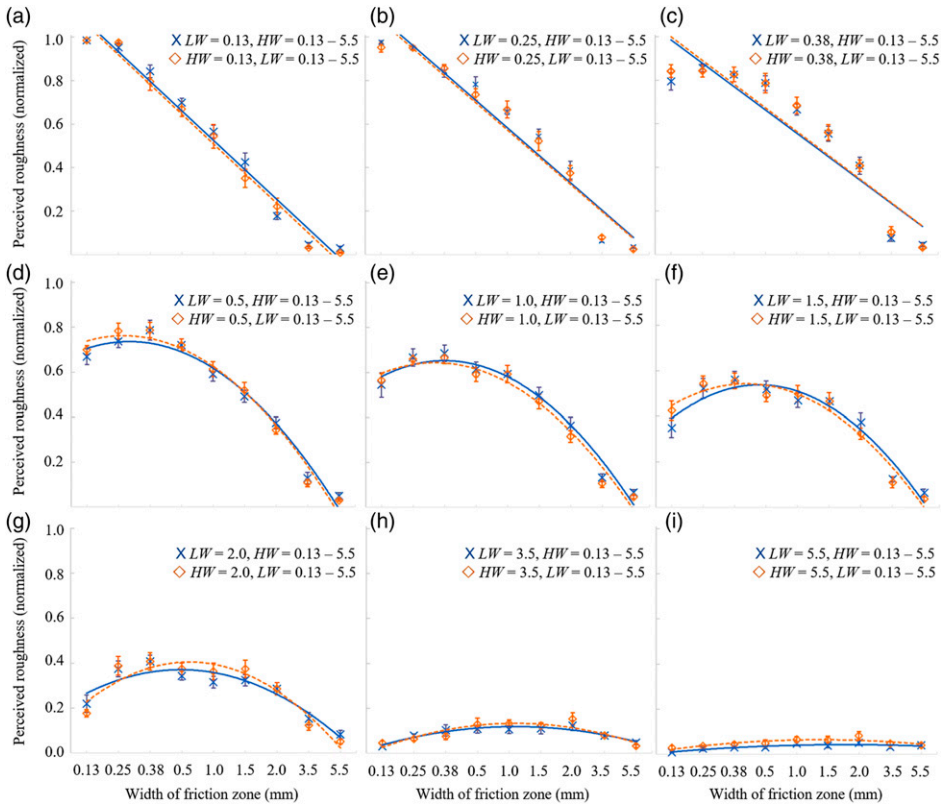

Figure 3. Means of magnitudes of perceived roughness with different widths of low-/high-friction zones in nine groups. In each group, there are nine varying conditions. Perceived roughness (PR) with the width of friction zones (W) are fitted using linear or quadratic regressions. The error bars represent the standard error of the means.

respectively in Figure 3i)). The peak points were at 2.0 mm width. The statistical analysis confirmed that the perceived roughness on the peak point was significantly different from 0.13 mm and 5.5 mm (all $p < 0.05$).

In summary, the above analysis indicates that *LW* and *HW* conditions in each group generally showed a similar trend with comparable magnitude values of perceived roughness.

Low- and High-friction Zones Effects

To obtain a concrete statistical result of the effects of *low-* and *high-friction zones* on perceived roughness, we further analyzed all the (*L*, *H*) = (a, b) versus (*L*, *H*) = (b, a) pairs using Wilcoxon signed-rank test. We excluded 9 patterns with the same *LW* and *HW* values from the 81 patterns, and grouped the rest patterns into 36 pairs for comparisons. The test was set at a significance level of $\alpha = 0.05$. The results are shown in Table 1.

According to the analysis results, no significant difference was found for each pair (all $p > 0.05$). Therefore, based on the plot analysis in Figure 3 and the analysis of pair comparisons in Table 1, it is reasonable to conclude that perceived pattern roughness would not be significantly different by swapping *low-* and *high-friction* zones.

Pattern Selection Method. The above analysis shows that (*LW*, *HW*) = (a, b) could achieve similar perceived roughness as (*LW*, *HW*) = (b, a). Therefore, both (*LW*, *HW*) = (a, b) and (*LW*, *HW*) = (b, a) patterns can be merged into a single pattern using the following formula.

Table 1. The Wilcoxon signed-rank test results on the 36 pairs of (*L*, *H*) = (a, b) versus (*L*, *H*) = (b, a) pattern pairwise comparisons.

(0.13,0.25) vs. (0.25, 0.13)	**(0.13,0.38) vs. (0.38, 0.13)**	**(0.13,0.5) vs. (0.5, 0.13)**	**(0.13,1.0) vs. (1.0, 0.13)**	**(0.13,1.5) vs. (1.5, 0.13)**	**(0.13,2.0) vs. (2.0, 0.13)**	**(0.13,3.5) vs. (3.5, 0.13)**	**(0.13,5.5) vs. (5.5, 0.13)**	**(0.25,0.38) vs. (0.38, 0.25)**	**(0.25,0.5) vs. (0.5, 0.25)**	**(0.25,1.0) vs. (1.0, 0.25)**	**(0.25,1.5) vs. (1.5, 0.25)**
$z = -0.74$	$z = -0.24$	$z = -0.87$	$z = -0.16$	$z = -1.34$	$z = -0.24$	$z = -0.97$	$z = -1.65$	$z = -0.32$	$z = -1.03$	$z = -0.08$	$z = -0.15$
$p = 0.46$	$p = 0.81$	$p = 0.39$	$p = 0.88$	$p = 0.18$	$p = 0.81$	$p = 0.33$	$p = 0.10$	$p = 0.75$	$p = 0.31$	$p = 0.94$	$p = 0.88$
(0.25,2.0) vs. (2.0, 0.25)	**(0.25,3.5) vs. (3.5, 0.25)**	**(0.25,5.5) vs. (5.5, 0.25)**	**(0.38,0.5) vs. (0.5, 0.38)**	**(0.38,1.0) vs. (1,0, 0.38)**	**(0.38,1.5) vs. (1.5, 0.38)**	**(0.38,2.0) vs. (2.0, 0.38)**	**(0.38,3.5) vs. (3.5, 0.38)**	**(0.38,5.5) vs. (5.5, 0.38)**	**(0.5,1.0) vs. (1.0, 0.5)**	**(0.5,1.5) vs. (1.5, 0.5)**	**(0.5,2.0) vs. (2.0, 0.5)**
$z = -0.06$	$z = -1.33$	$z = -0.95$	$z = -0.34$	$z = -0.43$	$z = -0.71$	$z = -0.26$	$z = -1.43$	$z = -1.54$	$z = -1.02$	$z = -0.71$	$z = -1.38$
$p = 0.953$	$p = 1.82$	$p = 034$	$p = 0.74$	$p = 0.67$	$p = 0.48$	$p = 0.80$	$p = 0.15$	$p = 0.12$	$p = 0.31$	$p = 0.48$	$p = 0.17$
(0.5,3.5) vs. (3.5, 0.6)	**(0.5,5.5) vs. (5.5, 0.5)**	**(1.0,1.5) vs. (1.5, 1.0)**	**(1.0,2.0) vs. (2.0, 1.0)**	**(1.0,3.5) vs. (3.5, 1.0)**	**(1.0,5.5) vs. (5.5, 1.0)**	**(1.5,2.0) vs. (2.0, 1.5)**	**(1.5,3.5) vs. (3.5, 1.5)**	**(1.5,5.5) vs. (5.5, 1.5)**	**(2.0,3.5) vs. (3.5, 2.0)**	**(2.0,5.5) vs. (5.5, 2.0)**	**(3.5,5.5) vs. (5.5, 3.5)**
$z = -0.47$	$z = -1.12$	$z = -0.27$	$z = -1.63$	$z = -1.57$	$z = -1.28$	$z = -0.28$	$z = -1.26$	$z = -1.38$	$z = -0.46$	$z = -0.98$	$z = -1.38$
$p = 0.64$	$p = 0.23$	$p = 0.79$	$p = 0.10$	$p = 0.12$	$p = 0.20$	$p = 0.78$	$p = 0.21$	$p = 0.17$	$p = 0.65$	$p = 0.33$	$p = 0.17$

Table 2. Means of roughness magnitudes of the 45 patterns in descending order.

Patterns	Roughness	Patterns	Roughness	Patterns	Roughness
(0.13,0.13)	0.984	(0.13,1.0)	0.555	(0.5,3.5)	0.119
(0.13,0.25)	0.964	(0.25,1.5)	0.533	(1.5,3.5)	0.117
(0.25,0.25)	0.951	(0.5,1.5)	0.506	(0.38,3.5)	0.089
(0.25,0.38)	0.850	(1.0,1.5)	0.484	(3.5,3.5)	0.079
(0.38,0.38)	0.827	(1.5,1.5)	0.466	(0.25,3.5)	0.071
(0.13,0.38)	0.819	(0.38,2.0)	0.408	(2.0,5.5)	0.067
(0.38,0.5)	0.787	(0.13,1.5)	0.388	(1.0,5.5)	0.056
(0.25,0.5)	0.759	(0.25,2.0)	0.381	(1.5,5.5)	0.051
(0.5,0.5)	0.721	(0.5,2.0)	0.359	(5.5,5.5)	0.041
(0.13,0.5)	0.684	(1.5,2.0)	0.349	(3.5,5.5)	0.040
(0.38,1.0)	0.675	(1.0,2.0)	0.339	(0.5,5.5)	0.040
(0.25,1.0)	0.669	(2.0,2.0)	0.286	(0.13,3.5)	0.038
(0.5,1.0)	0.602	(0.13,2.0)	0.198	(0.38,5.5)	0.038
(1.0,1.0)	0.592	(2.0,3.5)	0.138	(0.25,5.5)	0.030
(0.38,1.5)	0.558	(1.0,3.5)	0.119	(0.13,5.5)	0.019

$$(L, H) = \begin{cases} (\text{a}, \text{b}), & a \le b \\ (\text{b}, \text{a}), & a > b \end{cases} \quad (2)$$

where a and b represent one of the nine width values.

Consequently, the 81 experimental grating patterns were merged into 45 distinct patterns using formula (2), that is, the 36 pairs in Table 1 (select one pattern from a pair) and the 9 patterns with equal *LW* and *HW* values. Table 2 shows the merged 45 patterns in descending order of roughness magnitudes.

User interface design based on tactile textures usually needs to rely on multiple levels of roughness to accommodate task needs. It is thus worth finding a way to select grating patterns with perceived roughness varying to the greatest extent, so that users could distinguish them with minimal effort. Therefore, we proposed the following method to select candidate patterns.

$$r = \frac{R_{max} - R_{min}}{n - 1} \quad (3)$$

$$R_i = R_{max} - r \times (i - 1), \ (1 < i < \text{n}) \quad (4)$$

Where R_{max} and R_{min} represent the maximum and minimum of roughness magnitude values respectively, n represents the number of patterns to be selected, r represents the step value for the next calculation. In formula (4), i represents the index of roughness magnitude to be selected, and R_i represents the selected roughness magnitude.

For example, we can adopt the following steps to select 6 grating patterns with perceived roughness varying to the greatest extent. According to Table 2, R_{max} is 0.984 and R_{min} is 0.019, n is 6 for formula (3) and (4). Hence, r is equal to 0.193, R_1, R_2, R_3, R_4, R_5, and R_6 are calculated to be 0.984, 0.791, 0.598, 0.405, 0.212, and 0.019, respectively. The roughness magnitude of the selected patterns should be closed to the R_i values (i = 1, 2, 3, 4, 5, 6). According to Table 2, the corresponding patterns are set as (0.13, 0.13), (0.38, 0.5), (0.5, 1.0), (0.38, 2.0), (0.13, 2.0), (0.13, 5.5).

DISCUSSION

In this section, we discuss the experimental results against the two questions raised at the beginning of the experiment.

The first question aimed to explore the relationship between perceived roughness and varying widths of low-friction and high-friction zones. The data analysis reveals two trends of perceived roughness with varying widths of low-friction and high-friction zones. First, when *LW* or *HW* was set as constant values of 0.38 mm or lower, the perceived roughness generally

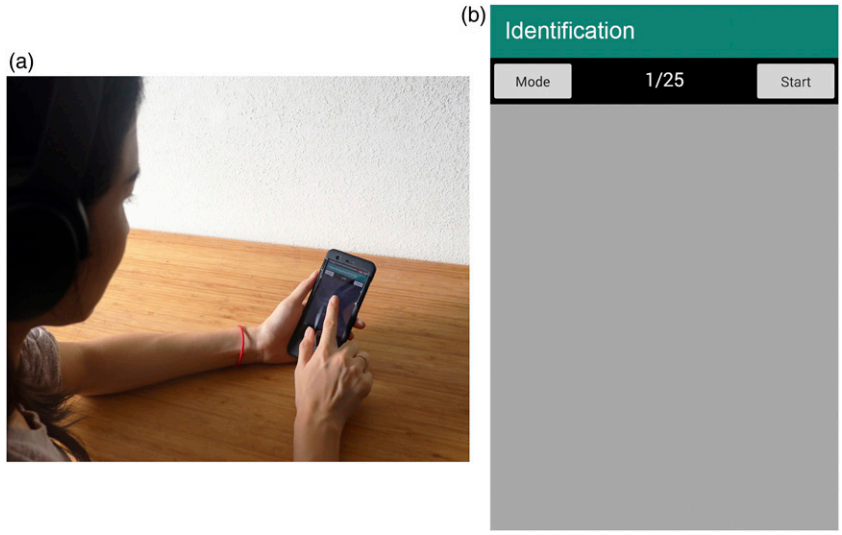

Figure 4. (a) Experimental environment and (b) interface for pattern identification tasks. In (b), the "Mode" button on the top of the interface was used to select a *pattern group* for the experiment. Clicking the "Start" button starts an identification trial, along with the text of the "Start" button changing to "Finish". Clicking the "Finish" button ends this identification trial and the text of the button changed to "Start" to indicate that participants can start the subsequent trial.

declined in a linear relationship with the increase of the width of the friction zone. Second, the perceived roughness followed an inverted U-shape trend when the constant factor of either *LW* or *HW* was larger than 0.5 mm but smaller than 2.0 mm. The inverted U-shape feature was in line with (Vardar et al., 2017); however, the peak point was shifted from 1.5 mm in (Vardar et al., 2017) to 0.38 mm in the present study. Such a difference may be due to different devices used in our study and the previous study.

In the second question, we aimed to look into if low-friction and high-friction zones would equally contribute to perceived roughness. The experimental results showed that low-friction and high-friction zones had similar effects on the perceived roughness. Such a conclusion was deduced from the result that swapping *low-* and *high-friction zones* had no significant effects on perceived roughness. In other words, when designing patterns such as (*LW*, *HW*) = (a, b), we can use the (*LW*, *HW*) = (b, a) pattern instead because both patterns could produce indistinguishable sensations for participants. To our knowledge, this is the first empirical evidence for understanding the simultaneous effects of *low-friction* and *high-friction* zones on perceived roughness.

EXPERIMENT 2: GRATING PATTERN IDENTIFICATION

With the pattern selection method proposed in Experiment 1, we can select a set of grating patterns with perceived roughness (*pattern group*) that would be most distinctive from each other. For example, as presented in *Identification Strategies*, the *pattern group* with 6 distinct patterns is (0.13, 0.13), (0.38, 0.5), (0.5, 1.0), (0.38, 2.0), (0.13, 2.0) and (0.13, 5.5). Following the identical method, we can obtain *pattern groups* with 2, 3, 4, 5, and 6 patterns. The goal of this experiment was to examine user performance in identifying the patterns in a given *pattern group*. We would like to address the following two questions.

Q1 What is the maximum number of patterns that participants could identify with high accuracy and short time? A larger sized *pattern group* could provide a richer design vocabulary; however, identification performance is likely to

Table 3. Selected patterns for the experiment. From the top to bottom, each row presents a *pattern group* with 2, 3, 4, 5, and 6 patterns, respectively. P1–P6 represent indexes of patterns in a *pattern group*. The numbers in the bracket above each image represent the magnitude of low- and high-friction zones, respectively.

Pattern group	Selected patterns					
2 patterns	P1 (0.13, 0.13)	P2 (0.13,5.5)				
3 patterns	P1 (0.13, 0.13)	P2 (0.5, 1.5)	P3 (0.13, 5.5)			
4 patterns	P1 (0.13, 0.13)	P2 (0.25, 1.0)	P3 (1.0, 2.0)	P4 (0.13, 5.5)		
5 patterns	P1 (0.13, 0.13)	P2 (0.25, 0.5)	P3 (0.5, 1.5)	P4 (2.0, 2.0)	P5 (0.13, 5.5)	
6 patterns	P1 (0.13, 0.13)	P2 (0.38, 0.5)	P3 (0.5, 1.0)	P4 (0.38, 2.0)	P5 (0.13, 2.0)	P6 (0.13, 5.5)

decline. Thus, it is worthy of finding out *pattern groups* with a large number of grating patterns while supporting fast and accurate identification performance.

Q2 How would participants behave when identifying patterns in *pattern groups* with different pattern numbers? Participants may adopt varying strategies to achieve fast and accurate identification performance. It is of interest to look into personalized strategies so as to gain insights into user behavior of identifying grating patterns.

Apparatus

The TPad phone in Experiment 1 was used in this experiment. The experiment application was developed in Java. The experimental environment and application interface are shown in Figure 4.

Participants

Twelve participants (6 male, 6 female) in the local university were recruited for the experiment. None of them participated in Experiment 1. The mean age of the participants was 20.8 years (SD = 0.75). All participants reported that they had at least four years of experience using touchscreen mobile devices, but none of them has used a tactile interface before, for example, the TPad. After the experiment, each of the participants was paid 50 Chinese yuan for their time.

Pattern Selection

Based on the pattern selection method in Experiment 1, we selected *pattern groups* with 2, 3, 4, 5, and 6 patterns for the experiment. The patterns are shown in Table 3.

We did not use *pattern groups* with more than 6 patterns because most of the participants had difficulty memorizing and identifying more than 6 patterns. Our pilot study showed that participants achieved an average accuracy rate lower than 60% when identifying 7 patterns.

Experiment Design

The experiment was a within-subject repeated measures design. The independent variables and dependent variables are as follows.

Independent variables: pattern groups with 2, 3, 4, 5, and 6 patterns, as shown in Table 3.

Dependent variables: identification accuracy (AC), reaction time (RT), and finger velocity. Identification accuracy was the ratio of the count of correct identified patterns to the number of trials. Reaction time was measured as the period from clicking the "Start" button to start a task until clicking the "Finish" button to complete the task. Finger velocity was the mean velocity of finger scanning on the touchscreen to perceive a pattern in a trial.

Tasks and Procedure

The experimental tasks were divided into five sessions. From the first to the fifth session, the participants needed to memorize and identify *pattern groups* with 2, 3, 4, 5, and 6 patterns respectively. Because participants were the first time to experience friction surface, the order of presentation of the five sessions was from easy

Table 4. Pattern-response normalized confusion matrices. (a)–(e) represent *pattern groups* with 2–6 patterns. P1–P6 are patterns indicated in Table 3.

		Identified	
2 patterns		**P1**	**P2**
Actual	**P1**	1.00	0.00
	P2	0.00	1.00

		Identified		
3 patterns		**P1**	**P2**	**P3**
Actual	**P1**	1.00	0.00	0.00
	P2	0.00	0.98	0.02
	P3	0.00	0.08	0.92

		Identified			
4 patterns		**P1**	**P2**	**P3**	**P4**
Actual	**P1**	0.97	0.03	0.00	0.00
	P2	0.03	0.92	0.05	0.00
	P3	0.00	0.20	0.80	0.00
	P4	0.00	0.00	0.08	0.92

		Identified				
5 patterns		**P1**	**P2**	**P3**	**P4**	**P5**
Actual	**P1**	1.00	0.00	0.00	0.00	0.00
	P2	0.07	0.82	0.08	0.03	0.00
	P3	0.00	0.20	0.75	0.05	0.05
	P4	0.00	0.00	0.22	0.73	0.05
	P5	0.00	0.00	0.00	0.18	0.82

		Identified					
6 patterns		**P1**	**P2**	**P3**	**P4**	**P5**	**P6**
Actual	**P1**	0.87	0.13	0.00	0.00	0.00	0.00
	P2	0.10	0.73	0.17	0.00	0.00	0.00
	P3	0.00	0.15	0.60	0.25	0.00	0.00
	P4	0.00	0.03	0.37	0.50	0.08	0.02
	P5	0.00	0.00	0.00	0.15	0.70	0.15
	P6	0.00	0.00	0.00	0.00	0.22	0.78

to hard, so as to allow for participants to ease gradually into the more complex patterns. In this way, we could avoid frustrating participants at the starting phase with difficult identification tasks, and make participants have the confidence to move on to the next task. Each session consisted of a practice phrase and a test phase. In the practice phase, the participants needed to experience the patterns of *pattern groups* in the session and practice identification tasks. The participants were instructed to wash their hands with soap to remove residual oils on the skin, and wore noise-canceling headphones to avoid the disturbance of audio clues on their answers.

Participants were asked to sit in a chair and perform the task with the index finger of the dominant hand while holding the device with the non-dominant hand. Once they were ready for the test, they clicked the "Start" button to start a trial and perceived the pattern on the TPad touchscreen (Figure 4b). When participants could identify the pattern, they needed to click the "Finish" button to complete the trial, and then reported their perceived pattern to the experiment moderator for record keeping. Participants were instructed to perform the task as quickly and accurately as possible. In a session, each pattern was repeated five times and all of the patterns were randomly shuffled during the session.

The experiment had (excluding practice trials): (2 patterns + 3 patterns + 4 patterns + 5 patterns + 6 patterns) × 5 repetitions × 12 participants = 1200 trials.

After the tasks, the experiment moderator discussed with the participants to collect their subjective feedback. The entire experiment lasted approximately 40 minutes for each participant.

RESULTS

We report the results in three aspects. First, we collected the pattern-response confusion matrices. Second, we calculated the overall performance of pattern identification. And third, we discussed the perception strategies that participants used to identify patterns.

Confusion Matrices

The pattern-response normalized confusion matrices of *pattern groups* with 2–6 patterns are shown in Table 4.

From the confusion matrices, we can find that the misidentified patterns were generally confused with their nearby patterns, and they usually had a lower level of perceived roughness. For example, for the *pattern group* with 4 patterns, the third pattern P3 was in most cases misidentified as the second pattern with the highest misidentification rate of 20%. Similarly, the fourth pattern (P4) in the *pattern group* with 5 patterns was misidentified as the third pattern with the highest rate of 22%. And for the *pattern group* with 6 patterns, the fourth pattern (P4) was misidentified as the third pattern (P3) with the highest rate of 37%.

The above results indicate that identification performance depends on grating pattern and the amount of patterns. Hence, we further analyzed the effects of grating patterns on identification performance. The Shapiro–Wilk test showed that accuracy (AC) and reaction time (RT) data were not all normally distributed and the Friedman test was used to analyze the results of each *pattern group*. The statistical results indicated that 3–6 patterns showed significant main effect on both AC and RT (3 patterns: $H(2) = 8.4, p < 0.02$ and $H(2) = 12.67, p < 0.01$ for AC and RT, respectively; 4 patterns: $H(3) = 8.33, p < 0.04$ and $H(3) = 11.29, p < 0.01$ for AC and RT, respectively; 5 patterns: $H(4) = 17.1, p < 0.01$ and $H(4) = 16.67, p < 0.01$ for AC and RT, respectively; 6 patterns: $H(5) = 13.89, p < 0.02$ and $H(5) = 18.28, p < 0.01$ for AC and RT, respectively). Whereas, the *pattern group* with 2 patterns showed no significant main effect on both AC and RT ($H(1) =$ null., $p =$ n.s. and $H(1) = 0.13, p = 0.25$ for AC and RT, respectively).

Post hoc analysis with Wilcoxon signed-rank test showed that low performance of AC and RT regularly occurred at patterns with low perceived roughness as shown in Table 5. For example, for the *pattern group* with 3 patterns, the lowest AC and longest RT occurred in P3 (0.13, 5.5) having the perceived roughness of 0.019. AC of P3 was significantly different from the other two patterns (all $p < 0.05$), whereas RT was significantly different from the P1 ($p < 0.05$). For the *pattern group* with 4 patterns, the lowest AC and longest RT occurred in P3 (1.0, 2.0) with the perceived roughness of 0.339. AC and RT of P3 were significantly different from P1 and P4 (all $p < 0.05$). For the *pattern group* with 5 patterns, AC and RT of P1 were significantly different from other patterns (all $p < 0.05$). Similarly, the *pattern group* with 6 patterns, P4 (0.38, 2.0) with the perceived roughness of 0.408 led to the lowest AC and longest RT. This pattern was significantly different from P1 in AC and RT (all $p < 0.05$).

Table 5. Results of *post hoc* pairwise comparison analysis with Wilcoxon signed-rank test on identification accuracy (AC) and reaction time (RT in seconds). Cells with gray background indicate significant effect ($p < .05$). P1–P6 are patterns in Table 3.

Pattern group	Patterns for pairwise comparison	AC values for the two patterns	*p*	RT values for the two patterns	*P*	Pattern group	Patterns for pairwise comparison	AC values for the two patterns	*p*	RT values for the two patterns	*P*
2 patterns	P1 vs. P2	1.0 vs. 1.0	n.s.	1.1 vs. 1.1	.94	3 patterns	P1 vs. P2	1.0 vs. .98	.32	1.6 vs. 2.3	.00
4 patterns	P1 vs. P2	.97 vs. .92	.26	1.9 vs. 2.2	.14		P1 vs. P3	1.0 vs. .98	.03	1.6 vs. 2.1	.03
	P1 vs. P3	.97 vs. .80	.03	1.9 vs. 2.8	.00		P2 vs. P3	.98 vs. .92	.04	2.3 vs. 2.1	.64
	P1 vs. P4	.97 vs. .92	.32	1.9 vs. 2.1	.05	6 patterns	P1 vs. P2	.87 vs. .73	.03	2.3 vs. .7	.03
	P2 vs. P3	.92 vs. 80	.07	2.2 vs. 2.8	.02		P1 vs. P3	.87 vs. .60	.01	2.3 vs. 2.9	.28
	P2 vs. P4	.92 vs. .92	1.0	2.2 vs. 2.1	.64		P1 vs. P4	.87 vs. .50	.01	2.3 vs. 3.3	.00
	P3 vs. P4	.80 vs. .92	.04	2.8 vs. 2.1	.02		P1 vs. P5	.87 vs. .70	.03	2.3 vs. 3.2	.02
5 patterns	P1 vs. P2	1.0 vs. .82	.01	1.8 vs. 2.4	.04		P1 vs. P6	.87 vs. .78	.10	2.3 vs. 2.8	.33
	P1 vs. P3	1.0 vs. .75	.00	1.8 vs. 2.8	.00		P2 vs. P3	.73 vs. .60	.15	2.7 vs. 2.9	.72
	P1 vs. P4	1.0 vs. 73	.02	1.8 vs. 2.7	.00		P2 vs. P4	.73 vs. 50	.07	2.7 vs. 3.3	.01
	P1 vs. P5	1.0 vs. .82	.01	1.8 vs. 2.4	.01		P2 vs. P5	.73 vs. .70	.75	2.7 vs. 3.2	.53
	P2 vs. P3	.82 vs. .75	.33	2.4 vs. 2.8	.04		P2 vs. P6	.73 vs. .78	.58	2.7 vs. 2.8	.64
	P2 vs. P4	.82 vs. .75	.47	2.4 vs. 2.7	.59		P3 vs. P4	.60 vs. .50	.16	2.9 vs. 3.3	.24
	P2 vs. P5	.82 vs. .82	1.0	2.4 vs. 2.4	1.0		P3 vs. P5	.60 vs. .70	.31	2.9 vs. 3.2	.31
	P3 vs. P4	.75 vs. .73	.72	2.8 vs. 2.7	.59		P3 vs. P6	.60 vs. .78	.09	2.9 vs. 2.8	.88
	P3 vs. P5	.75 vs. .82	.25	2.8 vs. 2.4	.06		P4 vs. P5	.50 vs. .70	.16	3.3 vs. 2.8	.34
	P4 vs. P5	.73 vs. .42	.42	2.7 vs. 2.4	0.2		P4 vs. P6	.050 vs. .78	.06	3.3 vs. 2.8	.16
							P5 vs. P6	.070 vs. .78	.06	3.2 vs. 2.8	.01

Identification Performance

We analyze the effects of *pattern groups* on identification performance in terms of accuracy, reaction time and finger velocity.

Identification accuracy. Accuracy data on the *pattern group* were normally distributed; thus, a repeated measure of ANOVA test was used to analyze the data. Results showed that there was a significant main effect on identification accuracy ($F_{4,\ 44} = 65.54$, $p < 0.01$). Generally, identification accuracy decreased as *pattern group* size increased as shown in Figure 5a. The mean accuracy rates were 100%, 96.67%, 90%, 82.33%, and 69.72% for *pattern groups* with 2, 3, 4, 5, and 6 patterns respectively. *Post hoc* with Bonferroni analysis showed that there were significant differences between *pattern groups* with 2 patterns and with 4–6 patterns (all $p < 0.05$). There was no significant difference between *pattern groups* with 2 patterns and 3 patterns ($p = 0.261$), and between 3 patterns and 4 patterns ($p = 0.295$). *Pattern group* with 6 patterns resulted in the lowest accuracy than other *pattern groups* (all $p < 0.05$).

Reaction time. *Reaction time* data on the *pattern group* were normally distributed; thus, a repeated measure of ANOVA test was used to analyze the data. Results showed that there was a significant main effect on reaction time for the *pattern group* ($F_{4,\ 44} = 65.54$, $p < 0.05$). As illustrated in Figure 5b, the reaction time generally increased as *pattern group* sizes increased. The mean reaction times were 1.07 s, 2.01 s, 2.23 s, 2.42 s, and 2.86 s for *pattern groups* with 2, 3, 4, 5, and 6, respectively. *Post hoc* analysis showed that participants needed significantly shorter times to identify a *pattern group* with 2 patterns than 3–6 patterns (all $p < 0.05$). However, there were no significant differences between each two *pattern groups* with 3, 4, 5, and 6 patterns (all $p > 0.05$).

Finger velocity. The Shapiro–Wilk test showed that velocity data were not all normally distributed and the Friedman test was used to analyze the results of each *pattern group*. There was no significant main effect for *pattern group* ($H(4) = 2.4$, $p = 0.663$). As shown in Figure 5c, the mean velocities were 44.5 mm/s, 44.1 mm/s, 48.6 mm/s, 52.1 mm/s, and 49.1 mm/s for *pattern group* size of 2, 3, 4, 5, and 6 patterns respectively.

Identification Strategies

To better understand how participants performed pattern identification, we collected participants' feedback after the experiment. There were mainly three strategies summarized as follows.

Perceived roughness strategy. Participants experienced a specific grating pattern and estimate its magnitude, then identified it from a group of patterns. This strategy was used by all the twelve participants for *pattern groups* with 2–6 patterns, and was particularly effective for *pattern groups* with 3 or fewer patterns, as shown in Figure 6. In general, when *pattern group* with 3 or fewer patterns all participants

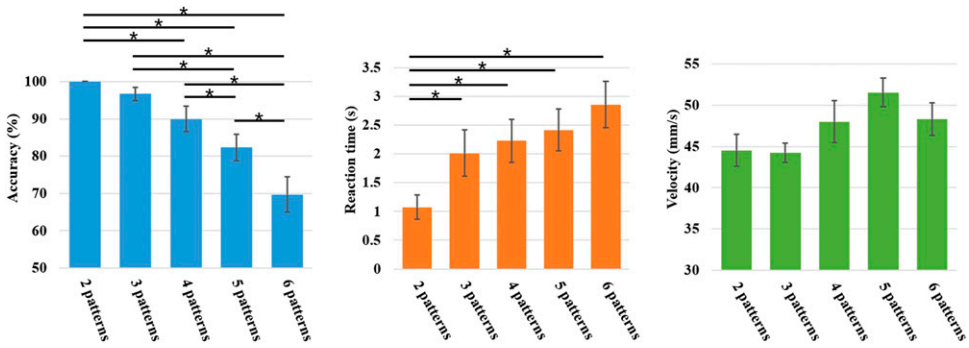

Figure 5. Performance of pattern identification on pattern group with 2–6 patterns in (a) identification accuracy, (b) reaction times, and (c) finger velocity. Error bars represent 0.95 confidence interval. (*: $p < 0.05$).

found it easy to identify the patterns. Participants could move their fingers from left to right once on the screen to experience a pattern for identification. The velocity of finger movement was approximately 41.9 mm/s. For *pattern groups* with 4–6 patterns, it was difficult for participants to just rely on perceived roughness to identify patterns with close perceived roughness. Only one participant reported that he just used perceived roughness to identify *pattern groups* with 2–6 patterns. He stated that identification became extremely difficult for a *pattern group* with 6 patterns and resulted in a low AC (57%).

Object association strategy. With this strategy, participants linked grating patterns to specific physical objects. For example, a large number of participants (91.7%) said that the (0.13, 0.13) pattern had a high perceived roughness and liked to associate it with the sensation of sandpapers, which could help them to quickly identify it from the other patterns. 33.3% of the participants linked the (0.25, 0.25) pattern to nail files as it gave them a strong level of roughness with dense bumpy sensation. Both (0.25, 0.5) and (0.25, 1.0) patterns were mapped to plastic combs as they provided the sensation of sliding one's finger on a dense comb (stated by 33.3% of the participants). The perceived roughness for (0.5, 1.5) and (0.5, 1.0) patterns were similar to smooth cotton (commented by 25% of the participants). One participant associated the (0.5, 1.0) pattern with a dense wheel spoke. 33.3% of the participants said they connected grating patterns to graphics patterns for identification. These object mappings enhanced the experience of touching specific patterns and helped participants increasing identification accuracy. 66.7%, 91.7%, and 91.7% of the participants used this strategy in identifying *pattern groups* with 4, 5, and 6 patterns respectively. All the participants said that identification became difficult for *pattern groups* with 5 or more patterns, particularly for the patterns with middle perceived roughness in the *pattern group*. To memorize those patterns, they must use multiple strategies to supplement the *perceived roughness* strategy. Also, participants needed to slide fingers left and right repeatedly on the screen to experience patterns multiple times to achieve correct identification. The velocity of finger motion was relatively high with a mean value of 50.1 mm/s.

Sensation comfort strategy. Participants grouped patterns into two clusters according to the level of comfort: pleasant and unpleasant ones. They then examined the patterns in each cluster

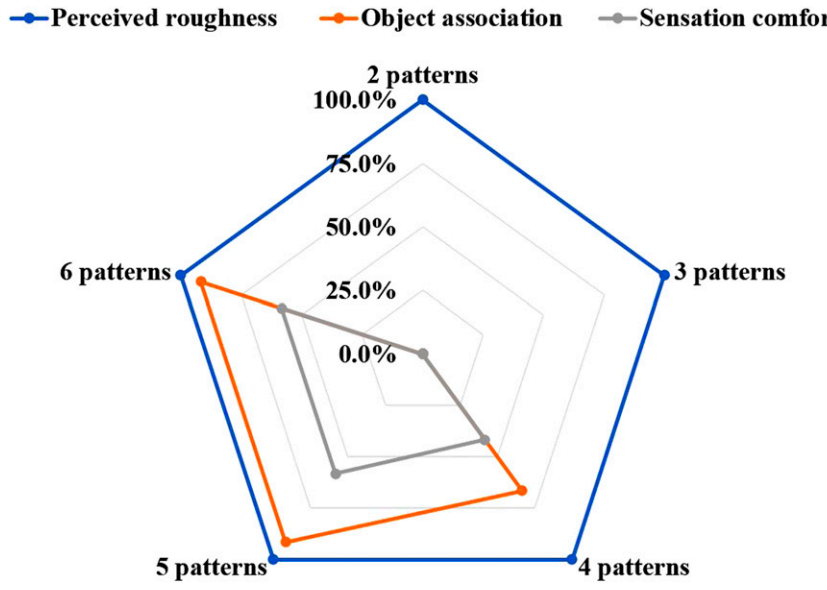

Figure 6. Percentage of identification strategies in *pattern group* with 2–6 patterns.

using the magnitude of perceived roughness or object association strategies. For example, they regarded (0.13, 2.0) and (2.0, 2.0) patterns as comfort patterns and assigned pleasant emotions to them, and regarded (0.13, 0.13) and (0.25, 0.25) as uncomfortable patterns and consider them as unpleasant emotions. 41.7%, 58.3%, and 58.3% of the participants used this strategy in identifying pattern groups with 4–6 patterns, respectively. It is worth noting that participants who used this strategy had used *object association* strategy as well. This sensation comfort strategy was in line with (Verrillo et al., 1999) suggesting that the pleasantness of the sensation decreased as perceived roughness increased.

Subjective feedback collected from the participants enabled us to understand better the sequence of strategies during the task. 41.7% of the participants had used the three identification strategies, and they had used the same sequence of the strategies. To identify grating patterns, they generally adopted the following three strategies in order. First, they usually used the method of *object association*, because it enabled the participants to do the task with the highest confidence. With this method, the participants could link grating patterns to real-world textures, so as to help memorize the patterns fast and identify them with high accuracy. If the *object association* method did not work, the participants then would use the *sensation comfort* strategy. This strategy could help participants classify patterns into smaller-size groups. If participants tried out the above two strategies without any results, they would use the strategy of *perceived roughness* to identify patterns. As participants used these strategies in sequence and stopped identification if they thought they succeeded, it is unlikely for them to have different results in an identification task.

DISCUSSION

In this section, we discuss the experimental results according to the two questions at the beginning of the experiment.

The first question was focused on the maximum number of patterns that participants could identify with high accuracy and short time. The experimental results showed that *pattern groups* with no more than 4 patterns could support pattern identification performance with high accuracy and short reaction time. *Pattern group* with 4 patterns (90%) had similar identification accuracy as *pattern group* with 3 patterns (96.67%), but significantly higher identification accuracy than *pattern group* with more than 4 patterns (82.3% for 5 patterns and 69.7% for 6 patterns). The identification accuracy for 5 patterns is similar to that revealed in the previous study (Rekik et al., 2017) (80.2%). In addition, the analysis of reaction time showed no significant difference between *pattern groups* with 3 patterns (2.01 s) and 4 patterns (2.23 s). Therefore, it should be reasonable to conclude that *pattern group* with 4 patterns is the maximum number that could support pattern identification performance with high accuracy and short reaction time.

We were also interested in the question of how would participants behave when identifying patterns in pattern groups with different pattern numbers. We found that participants generally depended on *perceived roughness*, *object association*, and *sensation comfort* strategies to identify patterns. The choice of identification strategies is subject to the number of patterns in the *pattern group*. For example, for *pattern groups* with 3 or fewer patterns, participants could use the *perceived roughness* strategy to identify patterns with ease. When *pattern group* with 4 or more patterns, participants additionally used *object association* and *sensation comfort* strategies to identify patterns. Rekik et al. have reported strategies for identifying tactile textures over a friction surface (Rekik et al., 2017), and our study further obtained new evidence on human behaviors in pattern identification in varying *pattern groups*.

GENERAL DISCUSSION

The experimental results have uncovered many notions regarding the effects of tactile grating patterns on perceived roughness for friction surface interaction design.

Understanding the Perceived Roughness

A significant finding of our study is no statistical differences between high and low-

friction zones in perceived roughness. This may be due to the fact that the frequency of multiple edges (i.e., periodic gratings that are composed by low-friction and high-friction zones) is the main factor affecting perceived roughness. The edges are produced by two types of consecutive step changes in friction: a step fall in friction (*FF*) followed by a step rise in friction (*RF*) or in the reverse order. The periodic gratings with these two types of step changes could contribute quite similar effects to perceived roughness. This explains why low- and high-friction zones resulted in similar perceived roughness. Such a result is in line with Saleem et al. (Saleem et al., 2020), which showed that period gratings displayed by consecutive sequences of *FF* followed by *RF* were perceived with the same acuity as compared to vice versa.

We compared the results of our study and Vardar et al. (Vardar et al., 2017) to gain insights into the effects of haptic devices on perceived roughness. While the haptic devices used in our study and Vardar et al's. (2017) are different (ultrasonic vs. electrostatic), the perceived roughness in both studies exhibited inverted U-shape trends with varying widths of low-friction and high-friction zones. This may be because the perceived roughness over virtual gratings depends on gratings' edges (Saleem et al., 2020) and the two device types could generate similar gratings' edges (E. Vezzoli et al., 2015).

However, the peak points in the inverted U-shape curves of perceived roughness in the two studies were different. This is may be due to the differences between the friction modulation techniques of the two haptic devices—ultrasonic haptic devices work by reducing friction, but electrostatic devices work by increasing friction. As a result, the two haptic devices would vary in the sharpness of virtual gratings' edges, leading to different peak points in the two studies. Other environmental factors such as finger moisture and contact temperature, the number of participants, and subject-to-subject variability such as the variability in fingerprints and finger electromechanical properties may also affect the results (Delhaye et al., 2014; Derler & Gerhardt, 2012; Derler et al., 2009; Pasumarty et al., 2011).

Our results indicated that perceived roughness generally declined linearly along with the increase of the width of the friction zone when *LW* or *HW* was set as a constant value of 0.38 mm or lower. When either *LW* or *HW* was set as a constant greater than 0.5 mm but less than 2.0 mm, the perceived roughness followed an inverted U-shape trend. The results differ from the studies on real textures, which showed that perceived roughness increased along with groove width increased (Hollins & Risner, 2000; Lawrence et al., 2007; Lederman, 1974). These differences may attribute to different texture generation mechanisms. Physical textures are generated by moving the finger over physical ridges and grooves on friction surfaces, but for virtual textures, perceived roughness is generated by widths of low- and high-friction zones.

Optimal *Pattern Group* Size

Existing studies have investigated pattern identification performance on friction surfaces (Potier et al., 2016; Rantala et al., 2009; Rekik et al., 2017). However, it is still unclear of the maximum *pattern group* size that participants could achieve high performance. Understanding the performance of tactile pattern identification is crucial in application design because different sizes of group patterns may lead to different identification performances. Accordingly, we proposed a method to form grating *pattern groups* with a number of patterns that are most distinctive from each other in terms of perceived roughness. In Experiment 2, we used this pattern selection method to determine five *pattern groups* and evaluated user performance of identifying the patterns in each group. From the results, we learned that the identification accuracy was greater than 90% when group sizes were 4 or less. Participants could identify the *pattern group* with 5 patterns in 82.3%. This result is comparable with (Rekik et al., 2017) which showed an accuracy of 80.2% when participants identifying 5 patterns. Participants could identify up to 6 patterns with an accuracy above 69.7%. This accuracy is better than (Saket et al., 2013) because it had an accuracy of 57% when participants identifying 6 patterns. These results explicitly determine the optimal *pattern group* size that supports optimal identification performance.

Design Implications

Our findings not only enrich the understanding of the perception of virtual textures on ultrasonic friction surfaces but also provide implications and recommendations for tactile interface design and applications.

1) Designing discriminable grating patterns should consider spatial period, and different width combinations of low- and high-friction zones. In general, denser patterns with lower widths of low- and high-friction zones provide higher perceived roughness than coarser ones. For example, patterns such as (0.25, 0.5) and (0.25, 1.0) could convey distinct sensations than those patterns with higher low- and high-friction zones such as (0.38, 2.0) and (1.0, 2.0). In addition, designers should avoid using (*LW*, *HW*) = (a, b) and (*LW*, *HW*) = (b, a) patterns as both could lead to a similar perceived roughness.
2) To form a group of patterns, our proposed method can be used to specify patterns with the most distinctive perceived roughness from each other. Our method can replace or complement other pattern selection methods such as the one using density (Klatzky et al., 2019).
3) Designers should suggest multiple perceptual strategies, such as perceived roughness, real object mapping and emotions, when an application requires users to identify a group of more than 4 patterns.

Applications of Interaction Design

Our results can support designing new tactile applications. One example is designing a target-approaching indicator on a tactile touchscreen. The linear trend of perceived roughness obtained in Experiment 1 could provide a smooth transition to the sliding finger, thus can be used to indicate the distance between the finger and the target. Another example is using a group of grating patterns to encode tactile alphabets. Experiment 2 proved that participants could identify a group of 4 grating patterns with high performance. Thus, designers could use 4 tactile patterns as code elements to efficiently encode tactile alphabets.

LIMITATIONS AND FUTURE WORK

Our work has several limitations. First, we measured texture perception in terms of perceived roughness of grating patterns and assessed identification performance on grating patterns. Future studies may consider other measurements (e.g., emotion state) to investigate the effects of tactile perception, and identification performance may vary by using multiple texture design strategies. Second, we aimed to investigate the fundamental factors of grating patterns and set static low- and high-friction widths in a specific grating pattern. This leaves room for future work to investigate dynamic rendering of grating patterns that the spatial period changes with finger velocity as presented in (Vezzoli et al., 2016). Third, our experiments were conducted on an ultrasonic frictional surface and future studies should further investigate user performance with other virtual texture actuation techniques such as electrostatic. Finally, we set the mean finger velocity as 50 mm/s by using an indicative moving cursor. This method might not provide high precise of finger velocity control. Future work should consider using high precise apparatus to control finger exploring speed.

CONCLUSIONS

In this study, we carried out two experiments to look into the effects of low- and high-friction zones on grating pattern design and also the human capability of identifying surface roughness. The main findings are below:

- Results of Experiment 1 show that perceived roughness was generally decreased along with the increase of either *LW* or *HW*. Trend analysis showed a strong linear effect when *LW* or *HW* was set as constant values of 0.38 mm or lower. Perceived roughness followed an inverted U-shape trend when the constant factor of either *LW* or *HW* was larger than 0.5 mm but less than 2.0 mm. The statistical analysis showed that the low- and high-friction zones had similar effects on human perception of roughness. According to the results, we proposed a pattern selection method to find patterns with the most distinctive perceived roughness from each other.

- Results of Experiment 2 indicate that participants could efficiently identify a *pattern group* with 4 patterns. They relied on *perceived roughness*, *object association*, and *sensation comfort* methods to identify grating patterns. Such empirical evidence provides necessary support for designing tactile interfaces such as tactile codes.

These findings help us obtain a comprehensive understanding of friction-based patterns and could provide implications for the design of efficient tactile applications over friction surfaces.

KEY POINTS

- Perceived roughness was generally decreased along with the increase of either *LW* or *HW* and followed linear or inverted U-shape trends.
- Participants could identify 4 or fewer grating patterns with high accuracy (>90%) and short reaction time (<2.2 s).
- Participants relied on *perceived roughness, object association* and *sensation comfort* methods to identify grating patterns.

DECLARATION OF CONFLICTING INTERESTS

The author(s) declared no potential conflicts of interest with respect to the research, authorship, and/or publication of this article.

FUNDING

The author(s) disclosed receipt of the following financial support for the research, authorship, and/or publication of this article: This work was sponsored by Grant No. LGF20F020001 from Public Projects of Zhejiang Province and No. 61502415 from the National Natural Science Foundation of China.

ORCID iD

Shaowei Chu https://orcid.org/0000-0001-5520-296X

SUPPLEMENTAL MATERIAL

Supplemental material for this article is available online. http://chushaowei.com/

REFERENCES

Basdogan, C., Giraud, F., Levesque, V., & Choi, S. (2020). A review of surface haptics: Enabling tactile effects on touch surfaces. *IEEE Transactions on Haptics*, *13*(3), 450–470. https://doi.org/10.1109/TOH.2020.2990712

Bateman, A., Zhao, O. K., Bajcsy, A. V., Jennings, M. C., Toth, B. N., Cohen, A. J., Horton, E. L., Khattar, A., Kuo, R. S., Lee, F. A., Lim, M. K., Migasiuk, L. W., Renganathan, R., Zhang, A., & Oliveira, M. A. (2018). A user-centered design and analysis of an electrostatic haptic touchscreen system for students with visual impairments. *International Journal of Human-Computer Studies*, *109*(1), 102–111. https://doi.org/10.1016/j.ijhcs.2017.09.004

Bau, O., Poupyrev, I., Israr, A., & Harrison, C. (2010). TeslaTouch: electrovibration for touch surfaces. In Paper presented at the Proceedings of the 23rd annual ACM symposium on User interface software and technology, New York, NY, 3–6, October 2010, pp. 283–292.

Biet, M., Casiez, G., Giraud, F., & Lemaire-Semail, B. (2008). Discrimination of virtual square gratings by dynamic touch on friction based tactile displays. In Paper presented at the 2008 Symposium on Haptic Interfaces for Virtual Environment and Teleoperator Systems, Reno, Nevada, USA, 13–14 March 2008, pp. 41–48.

Biet, M., Giraud, F., & Lemaire-Semail, B. (2007). Squeeze film effect for the design of an ultrasonic tactile plate. *IEEE Transactions on Ultrasonics Ferroelectrics and Frequency Control*, *54*(12), 2678–2688. https://doi.org/10.1109/TUFFC.2007.596

Birnholtz, J., Gergle, D., Liebman, N., & Sinclair, S. (2015). Feeling aware: Investigating the use of a mobile variable-friction tactile display for awareness information. In Paper presented at the Proceedings of the 17th International Conference on Human-Computer Interaction with Mobile Devices and Services, Copenhagen, Denmark, 24–27 August 2015, pp. 16–25.

Blake, D. T., Hsiao, S. S., & Johnson, K. O. (1997). Neural coding mechanisms in tactile pattern recognition: the relative contributions of slowly and rapidly adapting mechanoreceptors to perceived roughness. *Journal of Neuroscience*, *17*(19), 7480–7489. https://doi.org/10.1523/JNEUROSCI.17-19-07480.1997

Casiez, G., Roussel, N., Vanbelleghem, R., & Giraud, F. (2011). Surfpad: Riding towards targets on a squeeze film effect. In Paper presented at the Proceedings of the SIGCHI Conference on Human Factors in Computing Systems, Vancouver, BC, Canada, 7–12 May 2011, pp. 2491–2500.

Chen, C., Chua, S. H., Chung, D., Perrault, S. T., Zhao, S., & Kei, W. (2014). Eyes-free gesture passwords: a comparison of various eyes-free input methods. In Paper presented at the Proceedings of the Second International Symposium of Chinese CHI, Toronto, ON, Canada, 26–27 April 2014, pp. 89–92.

Connor, C. E., Hsiao, S. S., Phillips, J. R., & Johnson, K. O. (1990). Tactile roughness: Neural codes that account for psychophysical magnitude estimates. *Journal of Neuroscience*, *10*(12), 3823–3836. https://doi.org/10.1523/JNEUROSCI.10-12-03823.1990

Delhaye, B., Lefèvre, P., & Thonnard, J.-L. (2014). Dynamics of fingertip contact during the onset of tangential slip. *Journal of the Royal Society Interface*, *11*(100), 20140698. https://doi.org/10.1098/rsif.2014.0698

Derler, S., & Gerhardt, L. C. (2012). Tribology of skin: Review and analysis of experimental results for the friction coefficient of human skin. *Tribology Letters*, *45*(1), 1–27. https://doi.org/10.1007/s11249-011-9854-y

Derler, S., Gerhardt, L. C., Lenz, A., Bertaux, E., & Hadad, M. (2009). Friction of human skin against smooth and rough glass as a function of the contact pressure. *Tribology International*, *42*(11), 1565–1574. https://doi.org/https://doi.org/10.1016/j.triboint.2008.11.009

Gescheider, G. A., & Hughson, B. A. (1991). Stimulus context and absolute magnitude estimation: A study of individual differences. *Perception & Psychophysics*, *50*(1), 45–57. https://doi.org/10.3758/BF03212204

Gordon, M. L., & Zhai, S. (2019). Touchscreen haptic augmentation effects on tapping, drag and drop, and path following. In Paper presented at the Proceedings of the 2019 CHI Conference on Human Factors in Computing Systems, Glasgow, Scotland UK, 4–9 May 2019. No: 373, pp. 1–12. https://doi.org/10.1145/3290605.3300603

Gueorguiev, D., Vezzoli, E., Sednaoui, T., Grisoni, L., & Lemaire-Semail, B. (2019). The perception of ultrasonic square reductions of friction with variable sharpness and duration. *IEEE Transactions on Haptics*, *12*(2), 179–188. https://doi.org/10.1109/TOH.2019.2894412

Henderson, J., Avery, J., Grisoni, L., & Lank, E. (2019). Leveraging distal vibrotactile feedback for target acquisition. In Paper presented at the Proceedings of the 2019 CHI Conference on Human Factors in Computing Systems, Glasgow, Scotland, 4–9 May 2019, pp. 1–11. https://doi.org/10.1145/3290605.3300715

Hightower, B., Lovato, S., Davison, J., Wartella, E., & Piper, A. M. (2019). Haptic explorers: Supporting science journaling through mobile haptic feedback displays. *International Journal of Human-Computer Studies*, *122*(1), 103–112. https://doi.org/10.1016/j.ijhcs.2018.09.005

Hoggan, E., Brewster, S. A., & Johnston, J. (2008). Investigating the effectiveness of tactile feedback for mobile touchscreens. In Paper presented at the Proceedings of the SIGCHI Conference on Human Factors in Computing Systems, Florence, Italy, 5–10 April 2008, pp. 1573–1582. https://doi.org/10.1145/1357054.1357300

Hollins, M., & Bensmaa, S. J. (2007). The coding of roughness. *Canadian Journal of Experimental Psychology*, *61*(3), 184–195. https://doi.org/10.1037/cjep2007020

Hollins, M., & Risner, S. R. (2000). Evidence for the duplex theory of tactile texture perception. *Perception & Psychophysics*, *62*(4), 695–705. https://doi.org/10.3758/BF03206916

İşleyen, A., Vardar, Y., & Basdogan, C. (2020). Tactile roughness perception of virtual gratings by electrovibration. *IEEE Transactions on Haptics*, *13*(3), 562–570. https://doi.org/10.1109/TOH.2019.2959993

Jones, L. A., & Tan, H. Z. (2013). Application of Psychophysical Techniques to Haptic Research. *IEEE Transactions on Haptics*, *6*(3), 268–284. https://doi.org/10.1109/TOH.2012.74

Katz, D. (1989). *The World of Touch*. L. E. Krueger (Ed.). Taylor & Francis Ltd, Trans. L. E. Krueger

Klatzky, R. L., Nayak, A., Stephen, I., Dijour, D., & Tan, H. Z. (2019). Detection and identification of pattern information on an electrostatic friction display. *IEEE Transactions on Haptics*, *12*(4), 665–670. https://doi.org/10.1109/TOH.2019.2940215

Lawrence, M. A., Kitada, R., Klatzky, R. L., & Lederman, S. J. J. P. (2007). Haptic roughness perception of linear gratings via bare finger or rigid probe. *Perception*, *36*(4), 547. https://doi.org/10.1068/p5746

Lederman, S. J. (1974). Tactile roughness of grooved surfaces: The touching process and effects of macro- and microsurface structure. *Attention, Perception, & Psychophysics*, *16*(2), 385–395. https://doi.org/10.3758/BF03203958

Liu, X., & Dohler, M. (2020). Vibrotactile alphabets: Time and Frequency patterns to encode information. *IEEE Transactions on Haptics*, *14*(1), 161–173. https://doi.org/10.1109/TOH.2020.3005093

Luk, J., Pasquero, J., Little, S., MacLean, K., Levesque, V., & Hayward, V. (2006). A role for haptics in mobile interaction: initial design using a handheld tactile display prototype. In Paper presented at the Proceedings of the SIGCHI Conference on Human Factors in Computing Systems, Montréal, Québec, Canada, 22–27 April 2006, pp. 171–180. https://doi.org/10.1145/1124772.1124800

Mullenbach, J., Shultz, C., Colgate, J. E., & Piper, A. M. (2014). Exploring affective communication through variable-friction surface haptics. In Paper presented at the Proceedings of the SIGCHI Conference on Human Factors in Computing Systems, Toronto, ON, Canada, April 26–May 1, 2014, pp. 3963–3972.

Mullenbach, J., Shultz, C., Piper, A. M., Peshkin, M., & Colgate, J. E. (2013). Surface haptic interactions with a TPad tablet. In Paper presented at the UIST '13 Adjunct: Proceedings of the adjunct publication of the 26th annual ACM symposium on User interface software and technology, St. Andrews, Scotland, UK, 8–11 October 2013, pp. 7–8.

Pasumarty, S., Johnson, S., Watson, S., & Adams, M. J. T. L. (2011). Friction of the human finger pad: Influence of moisture, occlusion and velocity. *Tribology Letters*, *44*(2), 117–137. https://doi.org/10.1007/s11249-011-9828-0

Potier, L., Pietrzak, T., Casiez, G., & Roussel, N. (2016). Designing tactile patterns with programmable friction. In Paper presented at the IHM '16, Fribourg, Switzerland, 25–28 October 2016, pp. 1–7.

Rantala, J., Raisamo, R., Lylykangas, J., Surakka, V., Raisamo, J., Salminen, K., Pakkanen, T., & Hippula, A. (2009). Methods for presenting braille characters on a mobile device with a touchscreen and tactile feedback. *IEEE Transactions on Haptics*, *2*(1), 28–39. https://doi.org/10.1109/TOH.2009.3

Rekik, Y., Vezzoli, E., Grisoni, L., & Giraud, F. (2017). Localized haptic texture: A rendering technique based on taxels for high density tactile feedback. in Paper presented at the Proceedings of the 2017 CHI Conference on Human Factors in Computing Systems, Denver, Colorado, USA, 6–11 May 2017, pp. 5006–5015.

Saket, B., Prasojo, C., Huang, Y., & Zhao, S. (2013). Designing an effective vibration-based notification interface for mobile phones. In Paper presented at the Proceedings of the 2013 Conference on Computer Supported Cooperative Work, San Antonio, Texas, USA, 23–27 February 2013, pp. 1499–1504.

Saleem, M. K., Yilmaz, C., & Basdogan, C. (2020). Tactile perception of virtual edges and gratings displayed by friction modulation via ultrasonic actuation. *IEEE Transactions on Haptics*, *13*(2), 368–379. https://doi.org/10.1109/TOH.2019.2949411

Taylor, M. M., & Lederman, S. J. (1975). Tactile roughness of grooved surfaces: A model and the effect of friction. *Attention, Perception, & Psychophysics*, *17*(1), 23–36. https://doi.org/10.3758/BF03203993

Unger, B., Hollis, R., & Klatzky, R. (2011). Roughness Perception in Virtual Textures. *IEEE Transactions on Haptics*, *4*(2), 122–133. https://doi.org/10.1109/TOH.2010.61

Vardar, Y., İşleyen, A., Saleem, M., & Basdogan, C. (2017). Roughness perception of virtual textures displayed by electrovibration on touch screens. In Paper presented at the 2017 IEEE World Haptics Conference, Munich, Germany, 6–9 June 2017, pp. 263–268.

Verrillo, R. T., Bolanowski, S. J., & Mcglone, F. P. (1999). Subjective magnitude of tactile roughness. *Somatosensory & Motor Research*, *16*(4), 352–360. https://doi.org/10.1080/08990229970401

Vezzoli, E., Messaoud, W. B., Amberg, M., Giraud, F., Lemaire-Semail, B., & Bueno, M. (2015). Physical and

perceptual independence of ultrasonic vibration and electrovibration for friction modulation. *IEEE Transactions on Haptics*, *8*(2), 235–239. https://doi.org/10.1109/TOH.2015.2430353

Vezzoli, E., Sednaoui, T., Amberg, M., Giraud, F., & Lemaire-Semail, B. (2016). Texture rendering strategies with a high fidelity–Capacitive visual-haptic friction control device. In F. Bello, H. Kajimoto, & Y. Visell (Eds.), Haptics: Perception, Devices, Control, and Applications: 10th International Conference, EuroHaptics 2016, London, UK, 4–7 July 2016, Proceedings, Part I (pp. 251–260). Cham: Springer International Publishing.

Shaowei Chu is an associate professor in the College of Media Engineering at Communication University of Zhejiang, China. He received his PhD in computer science in 2013 from University of Tsukuba, Japan. His research area is Human-computer Interaction (HCI), with special interests in haptics interaction and user interface design.

Huawei Tu is a lecturer at La Trobe University, Australia. He is currently a visiting associate professor at CHEC in Kochi University of Technology, Japan. He received his PhD degree at Kochi University of Technology, Japan in 2012. He was a postdoc researcher at Ritsumeikan University of Japan from 2012 to 2013, and at Swansea University of the U.K. from 2013 to 2014. Before joining La Trobe University, he was an associate professor at Nanjing University of Aeronautics and Astronautics in China from 2014 to 2019. His research area is Human-computer Interaction (HCI), with special interests in multimodal interaction, user interface design and user experience design. He has published more than 30 research papers including top-tier HCI journal papers (e.g. ACM TOCHI) and conference papers such as ACM CHI.

Date received: December 14, 2021
Date accepted: November 7, 2021